

Computational Modelling and Comparative Analysis of a Schiff Base Ligand and Its Analog as Inhibitors Against Mild Steel Corrosion in 1M HCl

Chimezie Peter Ozoemena^{1*}, Ekerete Jackson Boekom¹, Godwin J Akpan², Itohowo Gabriel Asuquo³, Essien Kufre Edet⁴, Abai Ekaete Jacob⁵

¹ Department of Chemistry, Faculty of Science
University of Uyo, Uyo-520003, Akwa Ibom State, P.M.B. 1017, NIGERIA

² Department of Chemistry, College of Physical Science
Michael Okpara University of Agriculture, Umudike, Umuahia, Abia State, P.M.B. 7267, NIGERIA

³ Department of Chemistry, School of Science
Akwa Ibom State College of Education, Afaha Nsit, Etinan, Akwa Ibom State, P.M.B. 1019, NIGERIA

⁴ Department of Chemistry, Faculty of Physical Science
Akwa Ibom State University, Ikot Akpaden, Akwa Ibom, P.M.B. 1167, NIGERIA

⁵ Department of Chemistry
Akwa Ibom State Polytechnic, Ikot Osurua. Ikot Ekpene, 530102, Akwa Ibom, P.M.B 2100, NIGERIA

*Corresponding Author: chimexpex@gmail.com

DOI: <https://doi.org/10.30880/jsmpm.2024.04.01.007>

Article Info

Received: 29 March 2024

Accepted: 11 June 2024

Available online: 26 June 2024

Keywords

Adsorption, corrosion inhibition, schiff base ligand, synthesis

Abstract

Schiff bases, alternative anticorrosive additive was synthesized, characterized and investigated for the inhibition of mild steel corrosion in 1M Hydrochloric acid at concentrations of 20 ppm, 40 ppm, 60 ppm, 80 ppm and 100 ppm using weight loss (WL) and electrochemical methods. The novel Schiff base ligands obtained were characterized by Ultraviolet-visible and Fourier-Transform Infrared Spectroscopy. The elemental analysis data for the Schiff base ligands were used to confirm the general formula of the Schiff bases. Fourier-Transform Infrared spectroscopy provided evidence of formation of a complex surface film due to adsorption of the Schiff bases on the mild steel surface. Maximum inhibition efficiency for Schiff base ligand 1 (SBL1) and Schiff base ligand 2 (SBL2) obtained were respectively 76.92% and 86.21% at concentration of 100 ppm, and the trend followed SBL2>SBL1, indicating the effectiveness of SBL2 in corrosion prevention as compared SBL1. Potentiodynamic polarization (PDP) measurements showed that the Schiff bases acted as mixed type inhibitors. Electrochemical Impedance Spectroscopic (EIS) measurement revealed that the corrosion process was controlled by charge transfer process. Inhibition efficiency values obtained from the different techniques were comparable. Quantum chemical parameters such as highest occupied molecular orbital (HOMO), lowest unoccupied molecular orbital (LUMO) and energy gap (ΔE) were obtained using Hartree-fock Density Functional Theory by Hamiltonian method. The results showed that SBL2 was more reactive than SBL1. In conclusion, the inhibition of mild steel corrosion was due to adsorption of active molecules leading to formation of a protective layer on surface of mild steel.

1. Introduction

The importance of mild steel in chemical industry cannot be over-emphasized owing to its usefulness as structural material in several applications including construction of tanks, gas cylinders, pipelines, heat exchangers among others. This serves as basic tool for the industrialization and development of a nation [1-3]. Hydrochloric acid is a very important chemical widely used in certain industrial activities such as cleaning agent and acid descaling, as well as pickling of mild steel structures. Contact with this acid may cause damage to metal surface which must be controlled to avoid further deterioration due to corrosion [4-5]. The corrosion of mild steel is an electrochemical phenomenon that chemically involves the loss of electron from its surface. Corrosion as a highly destructive process negatively affects the performance of metallic materials applied in many construction sites. Moreover, their consequences are quite diverse and pose a great problem in the industries, construction and other civil services with adverse economic effect [6].

The annual cost of corrosion includes both direct and indirect costs that have a real impact on the gross domestic product (GDP) of many countries which spent billions of dollars in putting up their industries. Therefore, corrosion cost is not only calculated in terms of economic losses, but also includes system failures during various incidents such as oil spills in truck pipelines, canned food spills, traffic accidents caused by wear of bolts and nuts, environmental pollution, replacement of materials, and loss of lives and properties [7-11]. Conversely, efforts are being made by researchers to combat this menace by adoption of several options including electroplating, oiling, cathodic and anodic protection, and the addition of inhibitors. Inhibitors are often added during industrial processes so as to prevent metal dissolution from inorganic and organic acids which are often employed. Most effective and eco-friendly inhibitors are organic compounds (Schiff bases) that contain heteroatoms like nitrogen, sulfur, oxygen and phosphorus in a conjugated system. This unique structural property makes it easy for them to be absorbed on the metal surface and block the active site thereby reducing corrosion [12].

Schiff bases are usually synthesized from the condensation of primary amines and active carbonyl groups commonly used as anticancer, antituberculosis, anticonvulsant, antimalarial and antimicrobial [13] agents due to their intense biological activity. Schiff bases have also been studied as corrosion inhibitors, on various metals and in various environments, due to azomethine linkage [14]. The azomethine linkage and the donor atoms (N, S and O) in the back bone of the Schiff bases afforded stable complexes with various transition metals and are responsible for their biological activities and industrial application which can be altered depending on their structural diversity [15]. The influence of Schiff base compounds, on the corrosion of steel in acidic solution has been investigated by several researchers [16]. An investigation of novel Schiff base compound as corrosion inhibitor for mild Steel in 1.0 M HCl was reported by Haruna *et al.* [17]. In all acidic media, 4-(Pyridin-4-yl)thiazol-2-amine (PTA) showed forth better performance [18,19].

Computational technique has been used as a vital tool to evaluate organic inhibitors and predict their corrosion inhibition performances via quantum chemical calculations [20-21]. Through quantum chemical calculations, it is possible to obtain structural parameters, such as the energies of the frontier molecular orbitals, HOMO (highest occupied molecular orbital) and LUMO (lowest unoccupied molecular orbital), energy gap (ΔE), ionization energy (IE), electron affinity (EA), electronegativity (χ), global hardness (η), softness (S), the global electrophilicity (ω), dipole moment, and the fraction of electrons transferred (ΔN) [21]. These parameters influence the potential inhibition and are generally strongly correlated with the experimentally obtained inhibition efficiency [21].

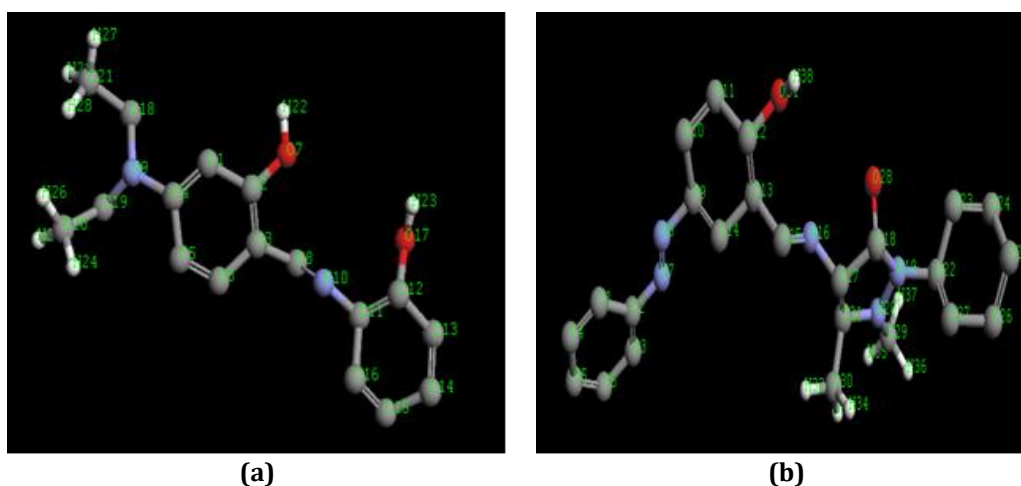


Fig. 1 Optimized structure (a) SBL1; (b) SBL2

The choice of these Schiff bases as inhibitors for this work stems from the fulfillment of the essential requirements of corrosion inhibitors, namely: possession of heteroatoms, presence of π -bonds/benzene ring, availability, cost effectiveness and friendliness to the environment. More so, it is expected that with the multiple adsorption sites, they shall be able to form complexes with the metal ions and on the metal surface. Hence, in this research work, due to the paucity of information on the inhibition potential of Schiff bases, the inhibitory properties of Schiff bases synthesized by reacting 4-aminophenol and 4-diethylamino-2-hydroxybenzaldehyde (SBL1), 4-amino antipyrine and 4-(Benzeneazo) Salicylaldehyde (SBL2) in 1M HCl solution on carbon steel is reported. The optimized geometry of SBL1 and SBL2 are shown in Fig. 1.

2. Materials and Method

2.1 Preparation of Specimens

The ASTM-A36 low carbon steel used in this research was obtained from Emma and Sons Nigeria limited, Okigwe, Imo State, Nigeria. The elemental composition of the mild steel by weight percentage was C – 0.17, Si – 0.26, Mn – 0.46, P – 0.0047, S – 0.017, Fe – 98.935. The ASTM-A36 low carbon steel specimens were mechanically pressed cut into coupons of dimension 4 x 3 x 0.017 cm³. With a progression of emery paper grades, from the coarsest to the finest, the coupons were polished using a variety of grades. The NACE recommended practice for surface finishing and cleaning of weight-loss coupons was followed when they were cleaned with distilled water, rinsed with absolute ethanol, and then dried in the open. Furthermore, coupons utilized in electrochemical investigations were mechanically cut into 1 cm x 1 cm coupons. The specimens' connecting terminals were embedded in epoxy resin, creating a 1 cm² working area. The surface preparation of the mechanically abraded specimens was carried out using silicon carbide emery paper of different grades (400 to 1200 grit) and subsequent cleaning with acetone and rinsing with distilled water prior to electrochemical measurement in 1 M HCl solution which was prepared by diluting 83 ml of 37% HCl (Merck) stock to 1 L standard flask with distilled water as corrosive environment. Finely polished low carbon steel was exposed to 1.0 M HCl in the presence and absence of inhibitors (SBL1 and SBL2). The solutions of the Schiff bases having the concentration of 20, 40, 60, 80 and 100 ppm were prepared.

2.2 Synthesis of Inhibitors

2.2.1 Synthesis of SBL1

The Schiff base ligand (SBL) was synthesized according to El-Lateef *et al* [24] with few modifications. 4-aminophenol (1.36 g, 0.01 mol) was added to a 30 mL magnetically stirred ethanolic solution of 4-diethylamino-2-hydroxybenzaldehyde (1.74 g, 0.01 mol) in a 100 mL round bottom flask (Fig. 2). 2.5 mL of glacial acetic acid was added to the mixture to adjust its pH (9.0) and then refluxed for 6 h upon which a bronze precipitate was formed instantly on cooling. The resulting precipitate was filtered, recrystallized with ethanol and dried in vacuum oven at 80 °C.

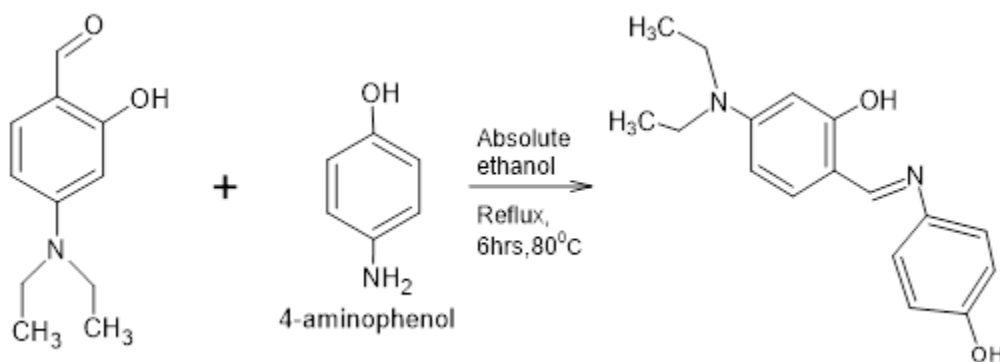


Fig. 2 Synthesis of SBL1 (C₁₇H₂₀N₂O₂)

2.2.2 Synthesis of SBL2

4-amino antipyrine (2.03 g, 0.01 mol) was added to a 30 mL magnetically stirred methanolic solution of 4-(Benzeneazo) Salicylaldehyde (2.08 g, 0.01 mol) in a 100 mL round bottom flask (Fig. 3). 1.5 mL of glacial acetic acid was added to the mixture, to adjust its pH and then refluxed for 4 h, upon which a teal green precipitate was formed instantly on cooling. The resulting precipitate was filtered, recrystallized with ethanol and dried in vacuum oven at 80 °C.

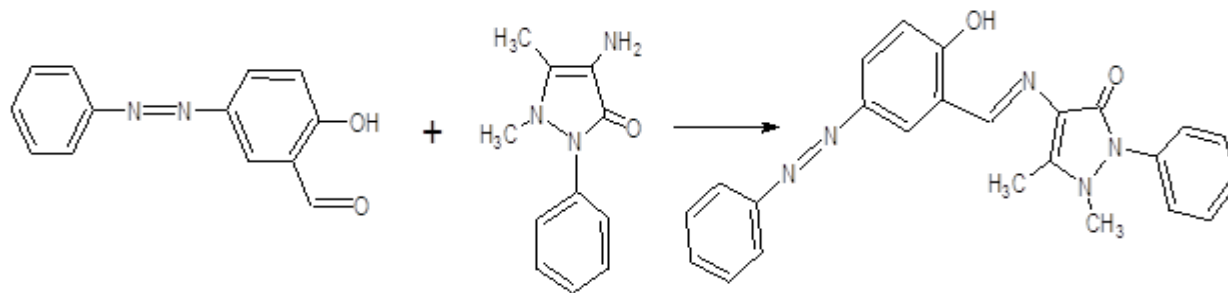


Fig. 3 Synthesis of SBL2 ($C_{24}H_{21}N_5O_2$)

2.3 Characterization on Inhibitors

2.3.1 Spectroscopic Determination of Functional Groups

The electronic absorption spectra also known as UV-Visible spectra are often very useful in determining the wavelength of maximum absorption (λ_{max}) and absorbance of the Schiff base ligands. Electronic spectra of the ligands were taken in absolute ethanol (10^3 cm^3) at scanned range of 300-800 nm on a UV-2500 PC spectrophotometer.

The IR spectra of the ligands were carried out for structural elucidation to determine the functional groups responsible for adsorption to the metal surface. For weight loss measurements, the coupons were dipped in 150 mL of 1.0 M HCl acid containing studied Schiff base ligands to form an adsorbed layer. The corrosion products were left for three days in 1.0 M HCl with and without 100 ppm of studied inhibitors, after which it's were retrieved, dried, and the films scraped. The films were collected and subjected to IR analysis [22]. The samples were prepared using KBr and the analysis were done by scanning the sample through a wave number range of $400\text{--}4,000 \text{ cm}^{-1}$ [21, 22].

2.3.2 Melting Point Determination

The melting points of the Schiff bases were determined by introducing a small amount of each sample (0.2 g) into a capillary tube and then inserted into Gallenkamp melting point Apparatus, the temperature at which the ligands melt was recorded after an average of two measurements.

2.4 Gravimetric Technique

100 ml each of the 1.0 M HCl solution were measured into six different beakers with one as the blank (uninhibited solution) and the remaining five labeled A to E containing different concentrations of the inhibitors ranging from 20 ppm to 100 ppm respectively. One mild steel coupon per beaker was used in each experiment. The test coupons were weighed before immersion in the acid solutions and the measurements were taken down. After weighing, the coupons were immersed in the acid solutions and then placed in a thermostatic water bath maintained at 303 K. The coupon in each beaker was noted to avoid mix up during the practical work. The immersion period was two hours' intervals, after two hours the coupons were retrieved from the acids, washed with tap water, degreased with ethanol and dried with acetone before the corresponding weights after immersion were recorded. The procedures were repeated for ten hours at 303K. The differences in weight of the coupons were again taken as the weight loss [22]. The corrosion rate (CR), inhibition efficiency (IE), and degree of surface coverage (θ) of mild steel in 1M HCl solution was computed using the formula:

$$\text{Corrosion rate (CR)} = \frac{\Delta W}{A \times T} \quad (1)$$

Where: ΔW = weight loss (g) given as $W_o - W_f$, W_o is the initial weight and W_f the final weight, A = total surface area of the test coupon (cm^2), T = immersion time (hours).

The Inhibition efficiency (IE) defines the level of performance of inhibitor that causes a decrease in corrosion rate. The inhibition efficiency (IE) was computed using the relationship in Equation 2 [23].

$$\%IE = \frac{(CR)_o - (CR)_{inh}}{(CR)_o} \times 100 \quad (2)$$

Where: $(CR)_o$ and $(CR)_{inh}$ are the corrosion rates in the absence and presence of different concentrations of the inhibitor, respectively. The surface coverage (θ) of the inhibitor was obtained from the experimental data using Equation 3 as follows:

$$\theta = \frac{(CR)_o - (CR)_{inh}}{(CR)_o} \quad (3)$$

Where: $(CR)_o$ = Corrosion rate in the absence of inhibitor, $(CR)_{inh}$ = Corrosion rate in the presence of inhibitor.

2.5 Electrochemical Measurements

The conventional three electrode set up was used consisting of saturated calomel electrode (SCE) as reference electrode (RE), platinum as counter electrode (CE) and mild steel coupons as working electrode (WE). The area of the WE exposed to the medium was approximately 1 cm². Fresh solution was used after each sweep. PDP measurements were carried out to obtain the information regarding the kinetics of the anodic and cathodic reaction on a mild steel surface. Before each PDP (Tafel) study, the electrode was allowed to corrode freely and its open circuit potential (OCP) was recorded as a function of time up to 1 hour which was sufficient to attain a stable state. After this, a steady state of OCP corresponding to the corrosion potential (E_{corr}) of the working electrode was obtained. PDP studies were conducted from cathodic to the anodic direction on the potential range ± 250 mV versus corrosion potential (E_{corr}) at a scan rate of 10 mV/s. Electrochemical Impedance Spectroscopy (EIS) measurements were used to confirm the aforementioned electrochemical behavior and to study the characteristic capacitive properties at the mild steel/solution interface. The EIS measurements were performed once the OCP was stabilized at a frequency range of 100KHz to 10 MHz with a signal amplitude perturbation of 5 mV. All electrochemical measurements were carried out at room temperature. The inhibition efficiency (%) from PDP was calculated from the measured I_{corr} values using Equation 4:

$$I(\%) = \left(\frac{I_{corr}^o - I_{corr}}{I_{corr}^o} \right) \times 100 \quad (4)$$

Where I_{corr}^o and I_{corr} are the corrosion current densities in the absence and presence of inhibitor respectively. The constant phase element which is defined by Y_o and n has correlation with the impedance as follows:

$$Z_{CPE} = Y_o^{-1} (j\omega)^{-n} \quad (5)$$

Where Y_o is the CPE constant and n is the CPE exponent, $j = (-1)^{1/2}$ which is an imaginary number and ω is the angular frequency in rad/s. CPE was used to compensate for the deviation from ideal dielectric behavior arising from the roughness of the mild steel surface. The value of n can be used as a gauge of the heterogeneity or the coarseness of the working electrode surface. The double layer capacitance (C_{dl}) values were calculated from Equation 6.

$$C_{dl} = \frac{1}{\omega R_{ct}} = \frac{1}{(2\pi f_{max} R_{ct})} \quad (6)$$

Where ω is the angular frequency ($\omega = 2\pi f_{max}$), f_{max} is the frequency at which the imaginary component of the impedance is maximum. The inhibition efficiency acquired from the impedance spectroscopy measurements was calculated using Equation 7:

$$\%IE = \frac{R_{ct(inh)} - R_{ct}^o}{R_{ct(inh)}} \times 100 \quad (7)$$

Where $R_{ct(inh)}$ and R_{ct}^o are the charge transfer resistance in the presence and absence of inhibitor, respectively.

2.6 Computational Technique

Computational techniques were employed to provide support for the experimental findings and to elucidate the nature of the interaction between the inhibitor molecules and the surface of mild steel. Density Functional Theory (DFT) method is a popular quantum chemical calculation tool for probing into structures, reactivity and selectivity of chemical molecules [23]. DFT calculation were carried out on new Schiff base structures and optimized with Hartree-Fock/Density Functional Theory (HF-DFT) by Becke's three parameter exchange functional along with the Lee- Yang-Parr non local correlation functional (B3LYP) and 6-31G* basis set in gas phase [23,24]. The molecular properties of the descriptors estimated include the frontier molecular orbital (MO), HOMO (highest occupied molecular orbital), LUMO (lowest unoccupied molecular orbital), energy band gap (ΔE), dipole moment (μ), electronegativity (χ), global hardness (η) and softness (σ) and fraction of electron transfer (ΔN) from inhibitors to metal surface using the following equation [24,25].

Ionization Energy (IE) and electron affinity (EA) the electronegativity (χ), global hardness (η) and softness (S), are defined in terms of the energy of the HOMO and the LUMO according to Koopman's theorem [24]. Ionization Energy (IE) is defined as the amount of energy required to remove an electron from a molecule [24]. It is related to the negative energy of the E_{HOMO} through the equation:

$$IE = -E_{\text{HOMO}} \quad (8)$$

Electron affinity [EA] is defined as the energy released when a proton is added to a system [24]. It is related to the negative energy of E_{LUMO} through the equation:

$$EA = -E_{\text{LUMO}} \quad (9)$$

The electronegativity (χ) is the measure of the power of an atom or group of atoms to attract electrons towards itself [38]. It can be estimated by using the equation:

$$\text{Electronegativity } (\chi) = \frac{IE + EA}{2} \quad (10)$$

Chemical potential (μ): The electronic chemical potential of a molecular (including atomic or ionic) species is the infinitesimal change in energy when electronic charge is added to it. We might define the electronic chemical potential as the negative of the electronegativity.

$$\text{Electronic chemical potential } (\mu): -\chi \quad (11)$$

Hardness (η) measures the resistance of an atom to a charge transfer [19]. It is estimated by using the equation:

$$\text{Hardness } (\eta) = \frac{IE - EA}{2} \quad (12)$$

Softness (σ) is the measure of the capacity of an atom or group of atoms to receive electrons [26]. Softness is the reciprocal of hardness. It is estimated by using the equation:

$$\sigma = \frac{1}{\eta} \quad (13)$$

The global electrophilicity (ω) index was introduced by Parr (1999) [35] as a measure of energy lowering due to maximal electron flow between donor and acceptor, and is given by the equation:

$$\text{Electrophilicity } (\omega) = \frac{\mu^2}{2} \sigma \quad (14)$$

Nucleophilicity (ϵ) is the reciprocal of electrophilicity expressed as:

$$\text{Nucleophilicity } (\epsilon) = \frac{1}{\omega} \quad (15)$$

Electron charge transfer (ΔN): The electron charge transfer evaluates the electronic flow in a reaction of two systems with different electronegativities, in particular an inhibitor molecule and a metallic surface. When there is a close contact between an iron and an inhibitor, electrons flow from lower electronegative (inhibitor) to higher electronegative (iron) until their chemical potentials (μ) or electronegativities (χ) become equal. The fraction of electrons transferred (ΔN) were calculated according to Pearson theory [25] by Equation 16:

$$\Delta N = \frac{\chi_{fe} - \chi_{inh}}{2(\eta_{fe} + \eta_{inh})} \quad (16)$$

While $\chi_{Fe} = 7\text{ eV}$ and $\eta_{Fe} = 0\text{ eV}$ are the theoretical values of electronegativity and hardness for iron.

3. Results and Discussion

3.1 Physicochemical Properties of the SBL

The physical properties of the synthesized Schiff bases were analyzed and presented in Table 1. The Schiff base ligands (SBL1 and SBL2) were prepared in good yield, coloured and air-moisture stable. The colour changes observed were confirmed by the electronic transition from lower to higher energy level. The melting point of SBL1 and SBL2 were found to be 187 °C and 192 °C which indicated that they were thermally stable ligands. The elemental analysis of the Schiff base ligands (SBL1 and SBL2) was also determined and the percentages of carbon, hydrogen and nitrogen in the compounds were set to be found (Table 1). The values obtained showed a reasonable agreement with the calculated values for the corresponding elements in all the Schiff bases (SBL1 and SBL2). The data for the Schiff bases suggested the formation of $C_{17}H_{20}N_2O_2$ for SBL1 and $C_{24}H_{21}N_5O_2$ for SBL2.

Table 1 Physical properties of the SBL

Compound	Molecular Formular	Colour	Yield (%)	Melting Point	Elemental Analysis		
					Calculated (Found)		
					C%	H%	N%
SBL1	$C_{17}H_{20}N_2O_2$ (284.37)	Bronze	74.63	187	71.80 (71.20)	7.04 (6.89)	9.85 (9.42)
SBL2	$C_{24}H_{21}N_5O_2$ (411)	Teal Green	65.89	192	70.07 (70.62)	5.11 (5.82)	17.03 (17.86)

3.2 Absorbance and Wavelength of Maximum Absorption of the SBL

The wavelength of maximum absorption of the Schiff base ligands (SBL1 and SBL2) are given in Table 2. SBL1 showed two major bands at 238.5 nm (41928.72 cm^{-1}) and 306 nm (32679.74 cm^{-1}) while SBL2 showed three essential absorption bands at 249.5 nm (40080.16 cm^{-1}), 275.0 nm (36363.64 cm^{-1}) and 320.5 nm (31201.25 cm^{-1}). The band appearing at lower energy (238.5, 249.5 and 275.0 nm) is attributed to $n \rightarrow \pi^*$ transition due to the nonbonding electrons present on the nitrogen atom of the azomethine group ($-\text{HC}=\text{N}$) and the phenolic group. The band appearing at higher energy (306 and 320.5 nm) is due to $\pi \rightarrow \pi^*$ transition of the ligand centered transitions (LCT) of benzene ring [25,26].

Table 2 Electronic spectroscopic data for the SBL

Compound	λ_{max}	Assignment
SBL ₁	238.5	$n \rightarrow \pi^*$
	306.0	$\pi \rightarrow \pi^*$
SBL ₂	249.5	$n \rightarrow \pi^*$
	275.0	$n \rightarrow \pi^*$
	320.5	$\pi \rightarrow \pi^*$

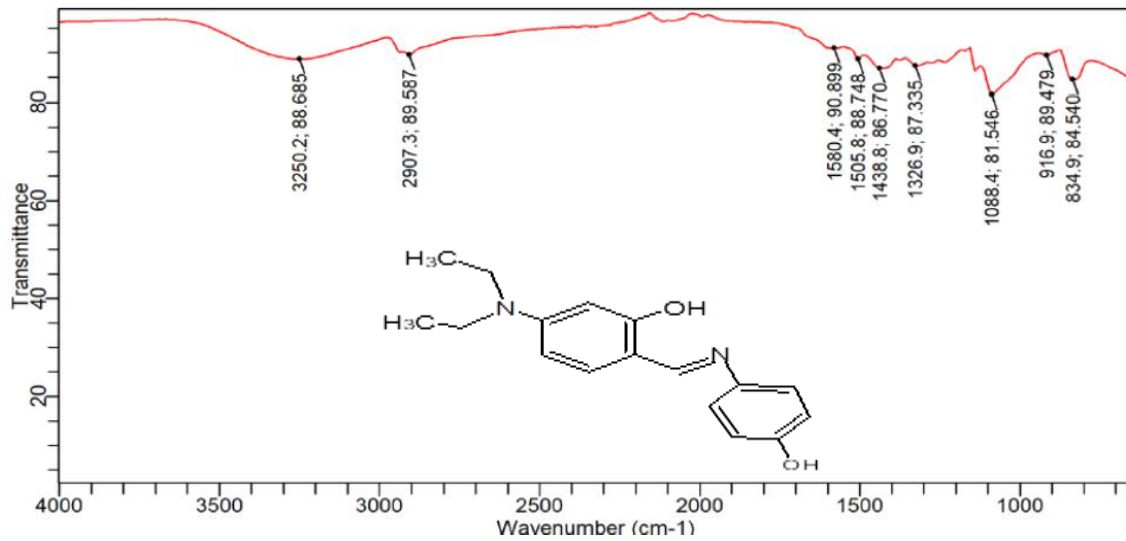
3.3 Fourier Transform Infrared Spectroscopy (FTIR) Analysis

The infrared absorption spectra of the Schiff bases and their corrosion products are presented in Table 3 by comparing the FTIR spectrum of the free Schiff base ligands (Fig. 4) with the spectra of the corrosion product in the presence of both SBL1 and SBL2 (Fig. 5), functional groups responsible for adsorption was deduced. From the results obtained, the azomethine stretch ($\text{C}=\text{N}$) at 1580.4 and 1617.7 cm^{-1} was shifted to 1625.1 and 1595.3

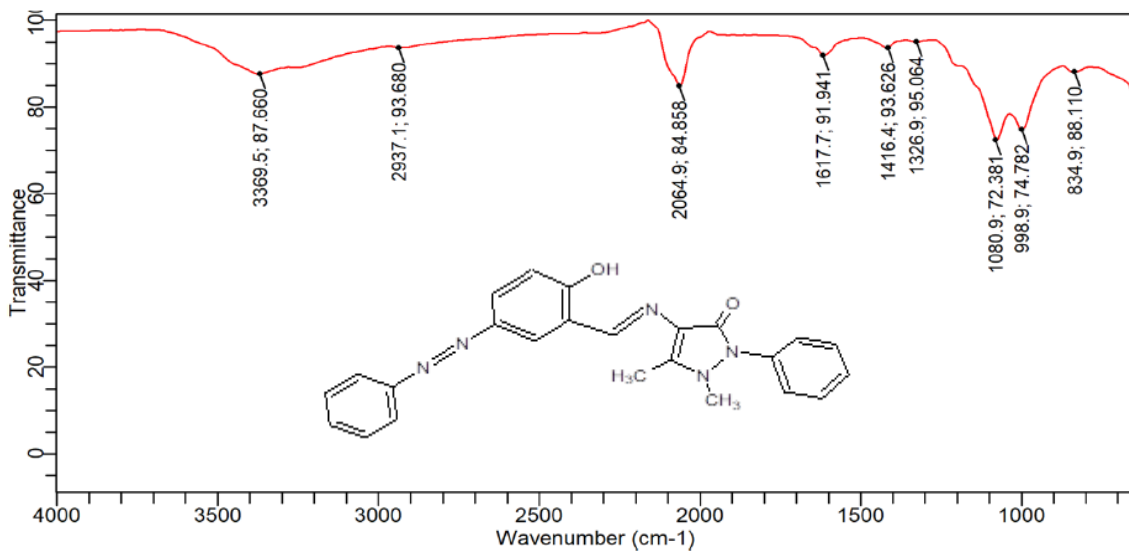
cm⁻¹. The shifts in frequencies of the various functional groups were responsible for the interaction between the mild steel surface and the Schiff bases while the missing and formations of new functional groups in the spectrum of the corrosion products indicated that these functional groups were used for the adsorption of the inhibitor onto the surface of the mild steel and facilitated the formation of novel chemical linkages as reported by Salman *et al.* (2019) [25]. Therefore, the preservation of metallic surfaces was achieved through the utilisation of functional groups found in the Schiff bases, namely SBL1 and SBL2.

Table 3 Relevant infrared spectra data for the SBL and its corrosion product

Compound	C-H	C-C	C-O	C-N	C=N	O-H	H ₂ O
SBL1	2097	1439	1327	1088	1580	3250	671.3
SBL2	2937	1417	1327	1081	1618	3370	671.3
SBL1 + MS	2922	1424	1329	1088	1625	3161	790.2
SBL2 + MS	2072	1491	1364	1096	1595	3116	693.3



(a)



(b)

Fig. 4 FTIR spectra (a) SBL1; (b) SBL2

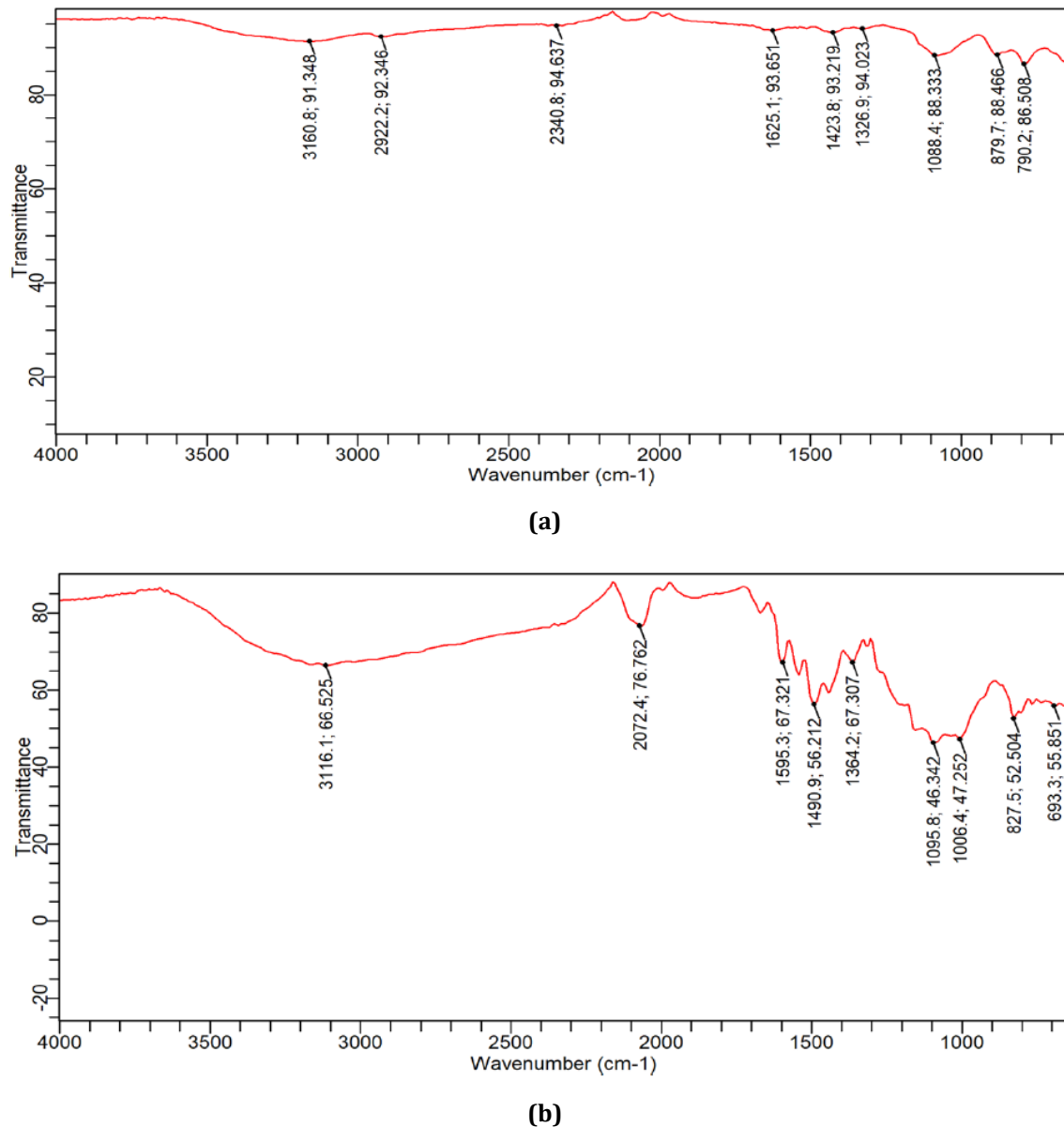


Fig. 5 FTIR spectra of the corrosion product of mild steel in the presence of (a) SBL1; (b) SBL2

3.4 Gravimetric Measurements

The corrosion rate of mild steel in the acidic medium containing the SBL2 exhibited a significant reduction compared to that in the presence of SBL1 (Fig. 6). This reduction can be attributed to the inhibitory properties exhibited by both Schiff bases as their concentrations increased. The trend of corrosion rate inhibition for the Schiff bases followed the sequence: SBL1>SBL2. This sequence underscores the effectiveness of SBL2 in preventing corrosion when compared to SBL1 inhibitor. The results are presented in Fig. 6. Similar results have been reported by Jamil *et al.* [26]. Furthermore, Fig. 7 also showed that the inhibition efficiencies of the Schiff bases in the test solutions increased with increase in concentrations of the inhibitor. Conversely, the inhibition efficiency of SBL2 (86.21 %) tend to be higher than SBL1 (76.92 %) at the various concentrations. Such remarkable performances may be due to the high molecular weight, the presence of abundant electron donation groups (C=O, O-H, N-H) and the presence of azomethine groups (HC=NR) [26].

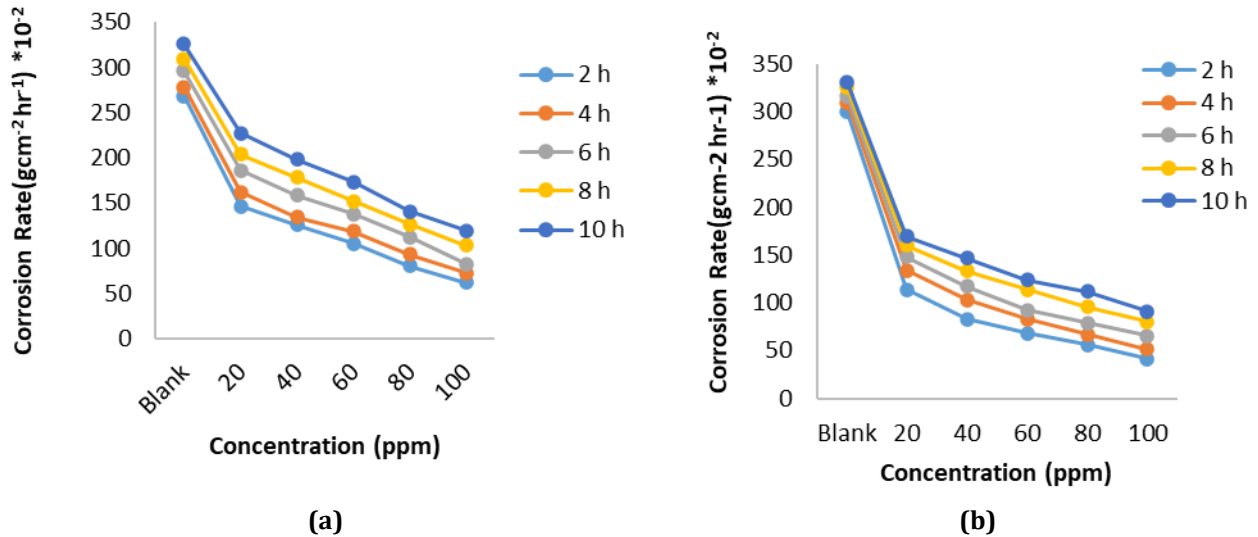


Fig. 6 Variation of corrosion rate with concentration for mild steel coupons in 1 M HCl solution at different time intervals (a) SBL1; (b) SBL2

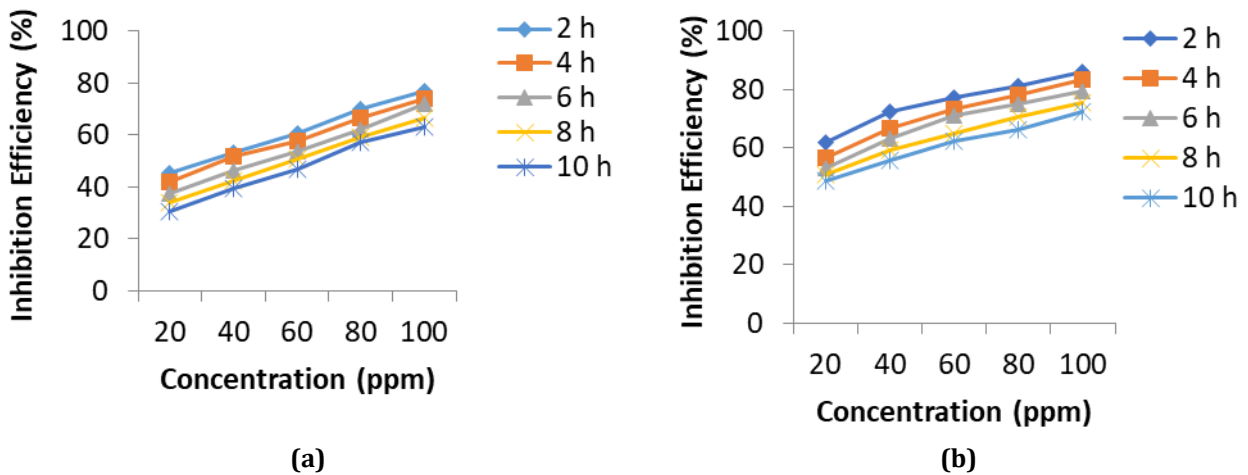


Fig. 7 Variation of inhibition efficiency with concentration at different time intervals (a) SBL1; (b) SBL2

3.5 PDP and Electrochemical Impedance Spectroscopic Measurements

The PDP parameters including corrosion current density (I_{corr}), potential (E_{corr}), cathodic and anodic constants (β_c and β_a), and inhibition efficiency (%) are presented in Table 4. In comparison to the free acid solution, the I_{corr} values exhibited a decrease with increasing inhibitor concentration. This phenomenon can be attributed to the formation of an adsorbed protective film consisting of the Schiff bases and their complexes on the surface of mild steel. Additionally, a shift of E_{corr} towards less negative values was observed in the presence of inhibitors compared to the free acid solution (Fig. 8). In general, corrosion inhibitors that cause a displacement of E_{corr} towards less negative values are categorized as anodic inhibitors, while those that shift the potential towards more negative values are regarded as cathodic inhibitors as reported by Jamil *et al.* [26] and Ituen *et al.* [27]. Consequently, the E_{corr} values obtained suggest that the inhibitors (SBL1 and SBL2) primarily affect the partial anodic and cathodic reactions. However, among the inhibitors, SBL2 demonstrate a greater influence. Thus, the addition of these inhibitors results in a further shift of the corrosion potential (E_{corr}) towards negative values. Nevertheless, this shift does not exceed -85 mV/SCE, making it challenging to categorize the Schiff base inhibitors as strictly cathodic or anodic. Typically, such corrosion inhibitors are considered mixed-type inhibitors with a prevalence of anodic inhibition [26,28].

The values of β_c and β_a , obtained upon the addition of the inhibitor, differ from those of the free acid solution (Table 4). The most significant difference was observed with β_a , indicating that the Schiff bases have a more substantial influence on the anodic reaction than the cathodic reaction. A mixed-type inhibitor operates by blocking some active sites involved in both the anodic and cathodic reactions of the metal without fundamentally altering its dissolution or corrosion mechanism. In other words, Schiff bases (SBL1 and SBL2) inhibit both the iron dissolution and hydrogen evolution processes, but are more active in inhibiting iron

oxidation (anodic reaction). Furthermore, the calculated inhibition efficiency increased with an increase in the concentration of the inhibitor consistent with the results obtained by Ituen *et al.* [27].

Table 4 PDP parameters for low carbon steel corrosion in 1 M HCl containing different concentrations of SBL1, ZnL1, NiL1 and CuL1

compound	Concentration (ppm)	$-E_{\text{corr}}$ (mV)	I_{corr} (μA)	β_c (V/dec)	β_a (V/dec)	$\eta\%$
SBL1	Blank (1M HCl)	472	905	65.10	113.70	-
	20	480	815	102.30	111.30	9.95
	100	486	689	105.50	124.20	23.87
SBL2	20	493	651	101.90	100.80	28.07
	100	500	518	124.50	106.90	42.76

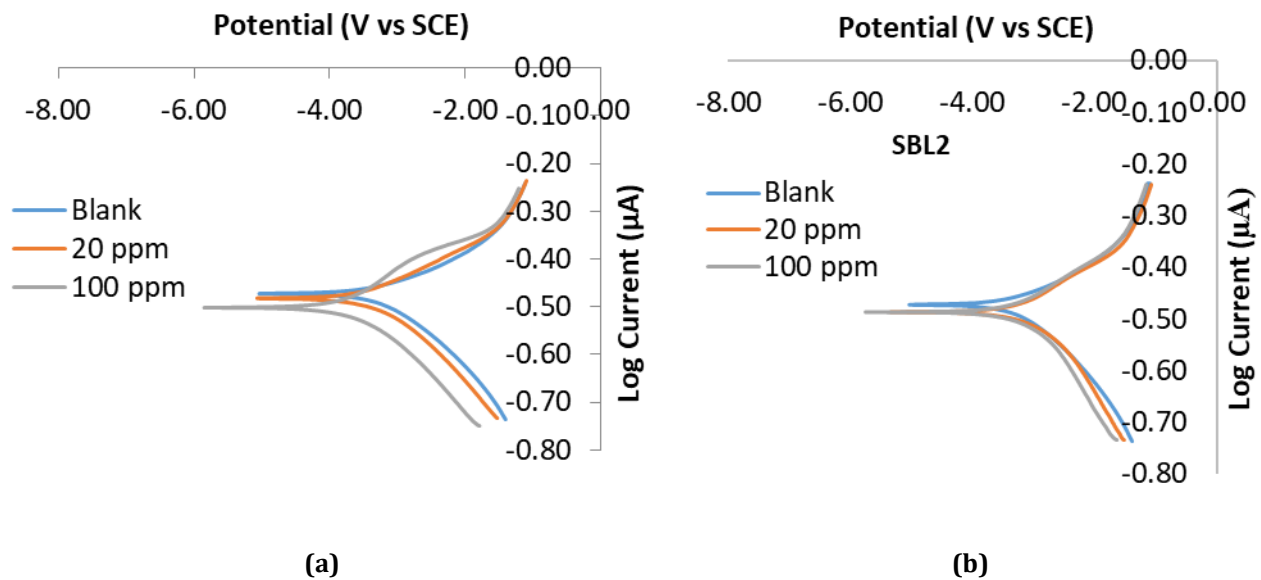


Fig. 8 Tafel plots for low carbon steel corrosion in 1 M HCl containing different concentrations (a) SBL1; (b) SBL2

EIS results for corrosion of mild steel in 1 M HCl in the absence and presence of SBL1 and SBL2 at room temperature were used to obtain Nyquist plots shown in Fig. 9. The presence of the Schiff bases (SBL1 and SBL2) influenced their diameters giving rise to an imperfect semicircle (Nyquist plot) as compared to the Blank (1 M HCl). As inhibitor concentration increased, the diameters also increased following the same trend as the calculated inhibition efficiency. However, the addition of SBL2 further increased the diameter of the capacitive loop (Fig. 9) compared to SBL1 which was attributed to its large molecular size and presence of more electron donating group giving rise to higher inhibition efficiency in SBL2.

Surface roughness of the mild steel is also responsible for the limitation in the shape of the semicircle. The charge transfer process obtained from the single capacitive loop mainly controlled the mechanism of corrosion [27]. Adjudged from the analogous shapes of the plots obtained for both inhibited and free acid solution, the mechanism of steel corrosion was not influenced by the introduction of SBL1 and SBL2. The equivalent circuit shown in Fig. 10 was used in the analysis of the Nyquist plots. This equivalent circuit was suitable for the modelling of mild steel dissolution in 1 M HCl solution in the absence and presence of the Schiff bases (SBL1 and SBL2) as shown by the values of goodness of fit (χ^2) (Table 5).

The EIS parameters derived from EIS plot (Fig. 9) are presented in Table 5. The value of n which decreased on addition of SBL1 and SBL2 described the extent of roughness or non-homogeneity of the steel surface suggesting that the adsorption of inhibitor molecules on steel surface active sites increased the surface roughness of the steel [27]. An increase in inhibitor concentration increased the charge transfer resistance showing that the 'blanketing' property of the film improved as inhibitor concentration increased. The control effectiveness obtained also developed with increase in inhibitor concentration, hence consistent with weight loss results. The inhibition efficiency increased progressively in the order SBL2>SBL1. The presence of inhibitors decreased C_{dl} values. Similar results were obtained by using fluvoxamine-based corrosion inhibitors [27] and pyridazine derivatives [34]. The decrease in C_{dl} values can be attributed to an increase in the thickness of the double layer or decrease in the local dielectric constant caused by the adsorbed protective film of the inhibitors as earlier inferred [28].

Table 5 EIS parameters for mild steel corrosion in 1 M HCl containing different concentrations of SBL1 and SBL2

EIS Parameters	HCl	SBL1		SBL2	
	1 M	20 ppm	100 ppm	20 ppm	100 ppm
R_{ct} (Ωcm^2)	19.52	115.40	183.10	202.30	356.31
R_s (Ωcm^2)	1.45	1.42	1.39	1.41	1.27
$\chi^2 \times 10^{-4}$	8.07	1.06	3.28	0.88	1.31
Y_{o1} ($\Omega\text{s}^n\text{cm}^{-2}$) $\times 10^{-4}$	3.36	2.43	2.13	2.57	2.00
$n_1 \times 10^{-1}$	8.64	8.33	8.12	8.29	8.08
R_f (Ωcm^2)	5.31	1.04	1.05	0.53	0.85
Y_{o2} ($\Omega\text{s}^n\text{cm}^{-2}$) $\times 10^{-2}$	6.42	1.95	1.06	5.28	1.94
$n_2 \times 10^{-1}$	1.98	1.86	1.71	0.95	0.61
C_{dl} (μF) $\times 10^{-2}$	8.15	1.38	0.87	0.79	0.66
$\eta\%$	-	83.09	89.34	90.11	94.52

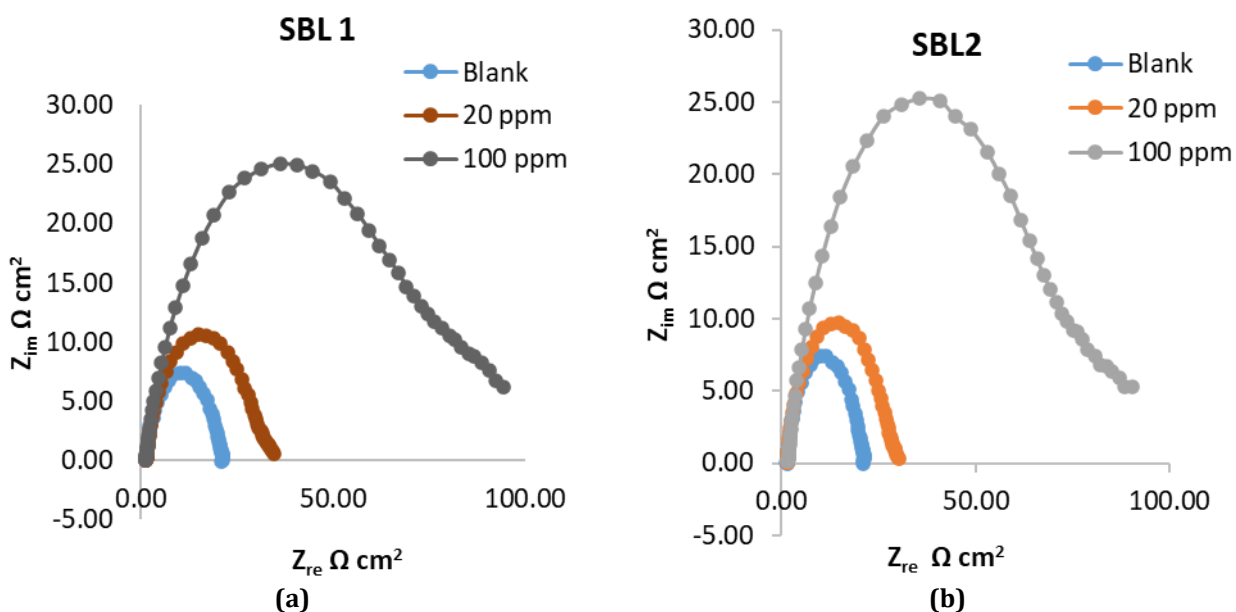


Fig. 9 Nyquist plot for inhibition of mild steel corrosion in 1 M HCl in the absence and presence (a) SBL1; (b) SBL2

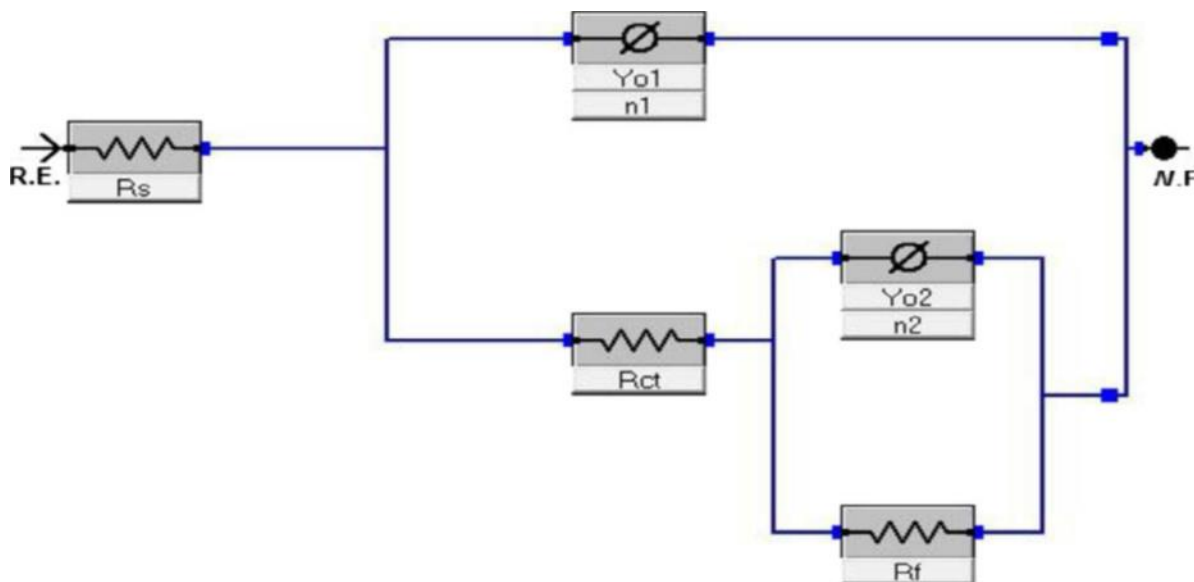


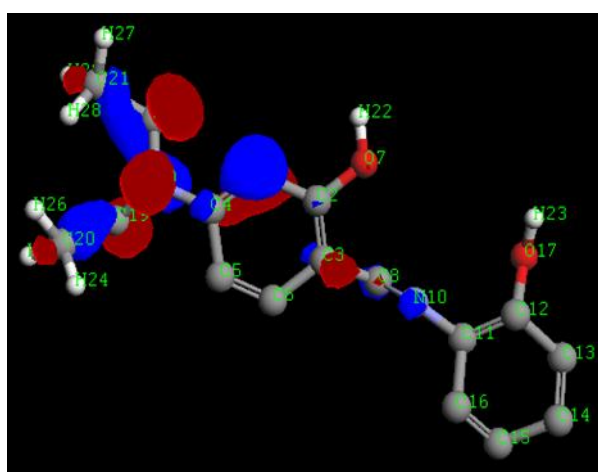
Fig. 10 Equivalent circuit used in the analysis of the impedance data

3.6 Computational Studies

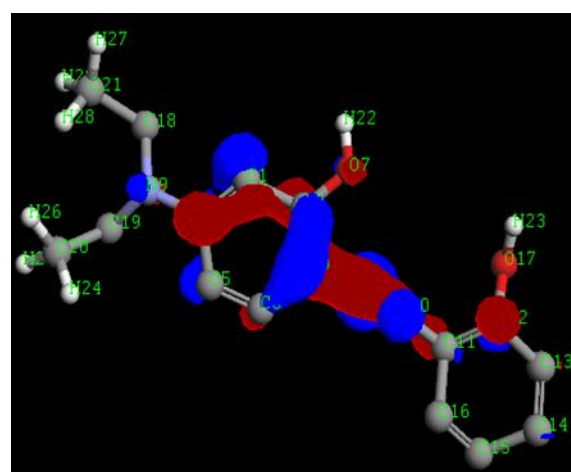
The positive and negative regions in HOMO and LUMO orbitals of the Schiff bases (SBL1 and SBL2) are shown in Fig. 11 and Fig. 12, respectively. The positive and negative phases of orbital are represented by two colours: blue regions represent an increase in electron density and red region represents a decrease in electron density [23]. From Fig. 11 to Fig. 12, it can be seen that the frontier orbitals: the HOMO and the LUMO were distributed all around each molecule most dominated by bonded heteroatoms (oxygen atoms and Nitrogen atoms of both amino and carboxylic groups) and some of the carbon atoms basically those containing unsaturated bonds in their molecule, and on the entire aromatic rings. These regions are the sites at which electrophiles attack and represent the active centers with the utmost ability to bond to the metal surface. The LUMO orbital can accept the electrons in the d-orbital of the metal using anti-bonding orbitals to form feedback bonds [28,29]. It has been reported that excellent corrosion inhibitors are usually those organic compounds that do not only offer electrons to unoccupied orbital of the metal, but also accept free electrons from the metal [29]. It is also well documented in literature that the higher the HOMO energy of the inhibitor, the greater its ability to offer electrons to unoccupied d-orbital of the metal, and the higher the corrosion inhibition efficiency. Although all compounds show comparable inhibition efficiency, SBL2 is more efficient inhibitor than SBL1 because of the presence of electron donating groups (methoxy substituent and azomethine) as evidenced from Table 6 that SBL2 has the highest value of E_{HOMO} (-5.1953 eV) and increased in the order: SBL2>SBL1 which suggest SBL2 would be better adsorbed on the metal surface than SBL1. E_{LUMO} represents the ability of the molecule to accept electrons from a donor reagent and the lower the value of E_{LUMO} , the greater the tendency of the molecule to accept electrons. Results from Table 6 also showed that SBL1 had the lowest value of E_{LUMO} (-1.0485 eV) and decreases in the order: SBL2 < SBL1 which suggested that SBL1 will readily accept electron from the metal than SBL2. The above assertion indicates that the Schiff bases are good corrosion inhibitor capable of donating electrons to the mild steel surface by forming an inhibition barrier [29]. This also confirms that the presence of these inhibitors increased their inhibition efficiency in line with the experimental results.

Table 6 Quantum chemical parameters of the SBL

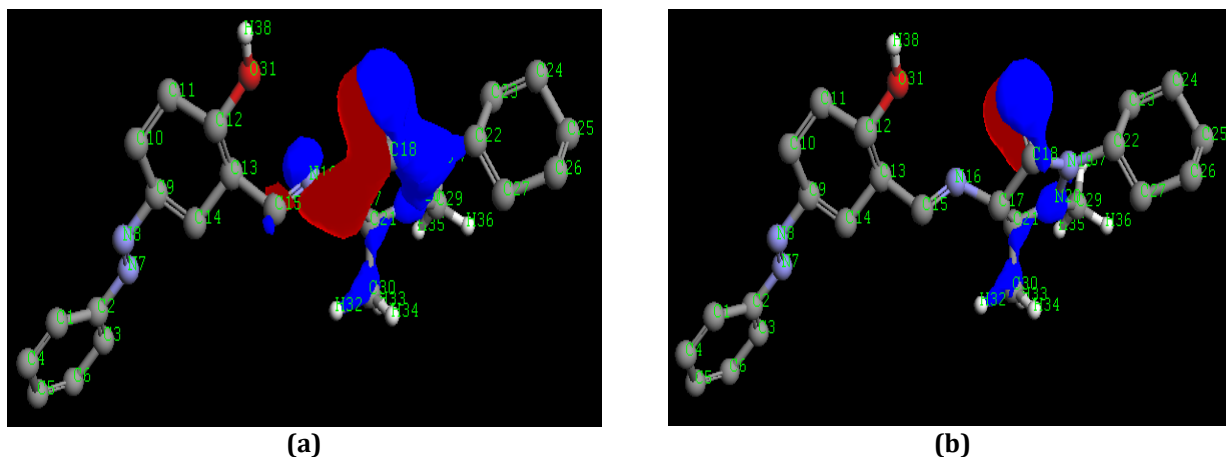
Parameters	Component	
	SBL1	SBL2
E_{HOMO} (eV)	-5.0002	-5.1953
E_{LUMO} (eV)	-1.0485	-1.8107
IE (eV)	5.0002	5.1953
EA (eV)	1.0485	1.8107
χ (eV)	3.5030	3.0244
η (eV)	1.9759	1.6923
σ (eV ⁻¹)	0.5061	0.5909
ω (eV)	3.6255	2.3147
ϵ (eV)	0.2758	0.4320
$\Delta E_{(\text{LUMO-HOMO})}$ (eV)	3.9517	3.3846
ΔN (eV)	1.0060	1.0332
μ (debye)	3.9047	4.2176



(a)



(b)

Fig. 11 Orbitals of SBL1(a) HOMO; (b) LUMO**Fig. 12** Orbitals of SBL2(a) HOMO; (b) LUMO

Apart from E_{HOMO} and E_{LUMO} , energy gap ($\Delta E = E_{\text{LUMO}} - E_{\text{HOMO}}$) is another essential quantum chemical parameter for explaining surface adsorptive behaviour of the inhibitor molecules. Generally, larger values of ΔE imply that the inhibition efficiency of the inhibitor is less due to low reactivity with the metal surface and lower values of ΔE imply that the inhibitor is having higher inhibition efficiency due to high reactivity with metal surface. Low values of the energy gap (ΔE) will provide good inhibition efficiencies because the excitation energy to remove an electron from the last occupied orbital will be low. A molecule with a low energy gap is more polarizable, and is generally associated with a high chemical reactivity, low kinetic stability and is termed soft molecule [30]. In this study, Table 6 shows the lower values of $\Delta E_{(\text{LUMO-HOMO})}$ in the following order SBL2 (3.3846 eV) < SBL1 (3.9517 eV). The adsorption of inhibitor onto a metallic surface occurs at the part of the molecule which has the greatest softness and lowest hardness [30].

Chemical hardness (η) and softness (σ) are significantly related to the band gap (HLG). The hard and soft acids as well as bases (HSAB) principle of Pearson requires that a reaction between an acid and a base is favoured when global softness difference is minimal [31]. These are important properties to measure the stability and reactivity of a molecule. Greater hardness therefore implies high stability and low reactivity. Global softness has an inverse relationship with hardness: soft molecules undergo changes in electron density more easily than the hard molecules, and are more reactive than the hard molecules [31]. A soft molecule has a small energy gap and a hard molecule has a large energy gap [31,32]. According to Pearson, hard molecules with large energy gaps cannot act as good corrosion inhibitors. Conversely, soft molecules with small energy gaps are efficient corrosion inhibitors because they can easily donate electrons to metal atoms at the surface. Table 6 reveals that the Schiff bases (SBL1 and SBL2) have lower values of softness (σ) and greater values of hardness (η). The softness (σ) values of the studied Schiff bases increased in the order: SBL2 (0.5909 eV) > SBL1 (0.5061 eV) and the corresponding hardness values decreased in the reverse form of the order: SBL2 (1.6923 eV) < SBL1 (1.9759 eV). This confirmed SBL2 as a more efficient corrosion inhibitor than SBL1 which is in agreement with the experimental inhibition efficiency results.

The electronegativity (χ), which is the negative of the chemical potential (μ), also indicates the propensity of an inhibitor molecule to accept electrons/electron density towards itself when cooperating with the metal atoms in a complex. The higher the electronegativity of a molecule, the stronger its adsorption on the metal surface. Table 6 shows the electronegativity of the Schiff bases in the order SBL1 > SBL2. This indicates that SBL1 has the highest value (3.5030 eV) and more tendency to accept electron from the metal making SBL1 and SBL2 an excellent corrosion inhibitor as both can donate and also accept electron concurrently, another conclusion in total agreement with the experimental finding.

The electrophilicity index (ω) is a quantum chemical descriptor that represents the propensity of an inhibitor molecule to accept an electron [32-33]. Table 6 also shows that the electrophilicity values of the Schiff bases range from 3.6255 to 2.3147 D^2/eV in the order SBL1 > SBL2. According to this descriptor, the electron-receiving capacity of SBL1 is significantly larger than that of the SBL2 molecule. For instance, the electrophilicity values for SBL1 and SBL2 are 3.6255 and 2.3147 D^2/eV , respectively. In other words, SBL1 has a high tendency to act as an electrophile while SBL2 has the high tendency to act as nucleophile. This trend is similar to those seen for the softness and electronegativity as revealed above. On the contrary, the nucleophilicity index (ϵ) is a quantum chemical descriptor that represents the propensity of an inhibitor molecule to donate an electron to the metal surface. Table 6 also reveals the order of nucleophilicity values as SBL2 > SBL1 which is the direct opposite of the electrophilicity arrangement. This trend is also in agreement with experimentally determined inhibition efficiency.

The dipole moment is another important quantum chemical parameter which gives information on the polarity of a molecule and therefore the distribution of electrons on the various atoms in the molecular structure. High value of dipole moment probably increases the inhibitor adsorption through the van der Waals type dipole-dipole forces [27,34]. In the study of corrosion inhibition, two different trends are often sighted correlating dipole moment with the inhibition efficiency (IE). Inhibition efficiency has been reported to increase with increase in the dipole moment of the inhibitor [35]. In other reports, inhibition efficiency has been reported to increase with the decrease in the dipole moment of the inhibitor [36]. Again, there are instances in which the dipole moment of the inhibitor has not shown any correlation to the inhibition efficiency of the inhibitor [37]. In this work, the order of inhibition efficiency is such that $SBL1 < SBL2$, as implicated by their energy gap (ΔE) which implies that inhibition efficiency increased with the increases in the dipole moment of the molecules as shown in Table 6 and followed the order: $SBL2 > SBL1$. The values of dipole moment in the above order also indicated the possibility of adsorption of studied inhibitors by electron donation to the unfilled d orbital of the metal [38].

The electron transferred (ΔN) is the propensity of a molecule to donate electrons and the greater the value of ΔN , the greater the propensity of a molecule to donate electrons to the electron poor species. Table 6 shows the number of electrons transferred (ΔN). According to Lukovits *et al.*, (2001) [39] if $\Delta N < 3.6$ the inhibition efficiency increased with increasing electron donating ability at the metal surface. It was also observed that the positive number of electrons transferred (ΔN) pointed out that the molecules act as an electron acceptor, while a negative number of electrons transferred (ΔN) indicated that the molecules acted as electron donors [31]. In the case of these molecules, values of ΔN are < 3.6 eV and are all positive suggesting that all the studied molecules are good electron acceptors, resulting in good inhibition efficiency. Thus, the highest fraction of electrons transferred was associated with the best inhibitor (SBL2), while the least fraction is associated with the inhibitor that has the least inhibition efficiency (SBL1).

Moreover, the mapping of molecular electrostatic potential (ESP) can allow an observation of the regions of high and low electron density in an organic corrosion inhibitor molecule. This can help determine the possible sites in the inhibitor molecule which are susceptible to undergo adsorption interaction with a metal surface [38-39]. The ESP mapping of the Schiff bases is displayed in Fig. 13. The different values of ESP are shown in different colours where the most negative ESP regions are shown in red colour (regions rich in electron), blue colour showed the region of the most positive ESP (electron deficiency) while the green colour showed the regions with zero ESP values [39-40]. It can be seen that in the Schiff bases, the most negative potential (red color) is around the heteroatoms (oxygen and nitrogen) and benzene rings which are predominate in SBL2. A deep blue coloured region can be observed around the carbon atoms of the inhibitors showing a deficiency of electrons and the possible centre susceptible to undergoing physical adsorption via electrostatic interaction. In SBL2 for instance, the red colour seen on the oxygen and nitrogen atoms indicate regions of high electron densities while the deep blue colour seen on the carbon atoms indicate regions of low electron densities. These results support the trends observed above in the values of the electrophilicity and the nucleophilicity indices (Table 6).

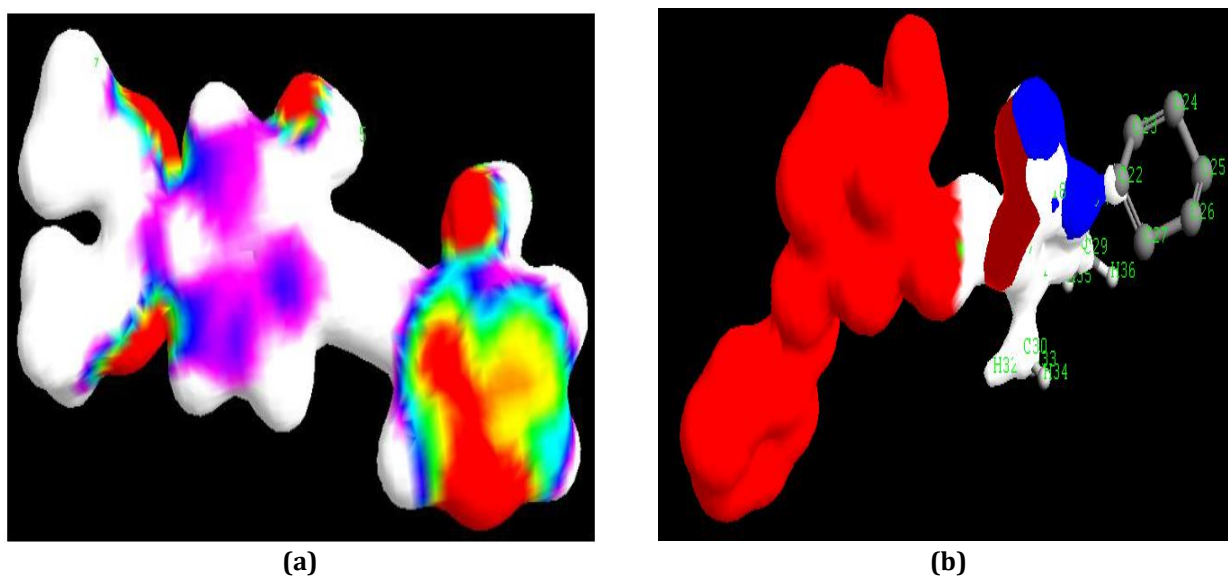


Fig. 13 ESP optimized mapped density (a) SBL1; (b) SBL2

4. Conclusion

The SBL1 and SBL2 were successfully synthesized and characterized by UV-Visible, FTIR and CHN-elemental analysis to affirm the proposed structure of the compound. The corrosion inhibition properties of the Schiff bases for mild steel in 1 M HCL solution were investigated. From the results obtained, it can be concluded that all the studied Schiff bases acts as an effective corrosion inhibitor for mild steel in 1M HCl acid solution and their inhibition efficiency increased with increase in the concentration of the Schiff bases with maximum efficiency obtained at an optimum concentration of 100 ppm within the first 2 hours. The electrochemical data were in strong agreement with the chemical data as all the studied Schiff bases increased the charged transfer resistance, reduced both the double layer capacitance and corrosion current densities of the interface. Values of E_{corr} also suggested that the Schiff bases acted as mixed type of inhibitors for mild steel. Hence, Weight loss measurements and electrochemical measurements (PDP and EIS) revealed SBL1 and SBL2 as excellent inhibitor for mild steel corrosion in 1M HCl. The parameters obtained from DFT-based quantum chemical computations was used to theoretically model the physisorptive interactions between the Schiff base molecules and the mild steel surface. The computational parameters obtained strongly suggested that the Schiff base molecules possess a high propensity for adsorption, underscoring their effectiveness as corrosion inhibitors for mild steel in a corrosive 1 M hydrochloric acid solution.

Acknowledgement

The authors would like to express their sincere thanks and appreciation to the Tertiary Education Trust Fund (Tetfund) Nigeria for their financial support.

Conflict of Interest

Authors declare that there is no conflict of interests regarding the publication of the paper.

Author Contribution

*The authors confirm contribution to the paper as follows: **study conception and design:** Chimezie Peter Ozoemena, Ekerete Jackson Boekom; **data collection:** Chimezie Peter Ozoemena; **analysis and interpretation of results:** Chimezie Peter Ozoemena, Ekerete Jackson Boekom; **draft manuscript preparation:** Chimezie Peter Ozoemena, Ekerete Jackson Boekom, Godwin J Akpan, Itohowo Gabriel Asuquo, Essien Kufre Edet, Abai Ekaete Jacob. All authors reviewed the results and approved the final version of the manuscript.*

References

- [1] Berrissoul, A., Loukili, E., Mechbal, N., Benhiba, F., Guenbour, A., Dikici, B., ... & Dafali, A. (2020). Anticorrosion effect of a green sustainable inhibitor on mild steel in hydrochloric acid. *Journal of Colloid and Interface Science*, 580, 740-752.
- [2] Paul, P. K., & Yadav, M. (2020). Investigation on corrosion inhibition and adsorption mechanism of triazine-thiourea derivatives at mild steel/HCl solution interface: Electrochemical, XPS, DFT and Monte Carlo simulation approach. *Journal of Electroanalytical Chemistry*, 877, 114599.
- [3] Saraswat, V., & Yadav, M. (2020). Computational and electrochemical analysis on quinoxalines as corrosion inhibitors for mild steel in acidic medium. *Journal of Molecular Liquids*, 297, 111883-111905.
- [4] Khanna, R., Kalia, V., Kumar, R., Kumar, R., Kumar, P., Dahiya, H., ... & Kumar, H. (2024). Synergistic experimental and computational approaches for evaluating pyrazole Schiff bases as corrosion inhibitor for mild steel in acidic medium. *Journal of Molecular Structure*, 1297, 136845.
- [5] Basiony, N. E., Elgendy, A., Nady, H., Migahed, M. A., & Zaki, E. G. (2019). Adsorption characteristics and inhibition effect of two Schiff base compounds on corrosion of mild steel in 0.5 M HCl solution: experimental, DFT studies, and Monte Carlo simulation. *RSC advances*, 9(19), 10473-10485.
- [6] Ugi, B. U., Obeten, M. E., Basse, V. M., Hitler, L., Adalikwu, S. A., Omaliko, C. E., ... & Uwah, I. E. (2022). Adsorption and inhibition analysis of aconitine and tubocurarine alkaloids as eco-friendly inhibitors of pitting corrosion in ASTM-A47 low carbon steel in HCl acid environment. *Indonesian Journal of Chemistry*, 22(1), 1-16.
- [7] Ozoemena, C. P., Boekom, E. J., & Akpan, I. (2023). Synthesis, Characterization and Electrochemical Studies on the Corrosion Inhibition Properties of Schiff Bases for Mild Steel in 1 M HCl Solution. *Chemical Science International Journal*, 32(2), 30-50.
- [8] Ganjoo, R., Sharma, S., Thakur, A., Assad, H., Sharma, P. K., Dagdag, O., ... & Kumar, A. (2022). Experimental and theoretical study of Sodium Cocoyl Glycinate as corrosion inhibitor for mild steel in hydrochloric acid medium. *Journal of Molecular Liquids*, 364, 119988.

- [9] Gergely, A. (2019). Phenomena and theories in corrosion science: methods of prevention. Nova Science Publishers.
- [10] Ozoemena, C. P., Boekom, E. J., Abai, E. J., Edet, E. K., & Akpan, I. A. (2023). Schiff Base and Its Metal Complexes as Ecofriendly Pitting Corrosion Inhibitors on ASTM-A36 Low Carbon Steel in Corrosive Oil and Gas Well Treatment Fluids. *Science Journal of Chemistry*, 11(5), 168-188.
- [11] Yang, X., Li, F., & Zhang, W. (2019). 4-(Pyridin-4-yl) thiazol-2-amine as an efficient non-toxic inhibitor for mild steel in hydrochloric acid solutions. *RSC advances*, 9(19), 10454-10464.
- [12] Jackson, E., Essien, K. E., & Okafor, P. C. (2016). Experimental and Quantum Studies: A New Corrosion Inhibitor for Mild Steel. *Elixir Corrosion and Dye*, 86, 34978-34983.
- [13] Haruna, A., Rumah, M. M., Sani, U., & Ibrahim, A. K. (2021). Synthesis, Characterization and corrosion Inhibition Studies on Mn (II) and Co (II) Complexes Derived from 1-[(Z)-[(2-hydroxyphenyl) imino] methyl] naphthalen-2-ol in 1M HCl Solution. *International Journal of Biological, Physical and Chemical Studies*, 3(1), 09-18.
- [14] Ohtsuka, T., Nishikata, A., Sakairi, M., & Fushimi, K. (2018). *Electrochemistry for corrosion fundamentals* (pp. 79-96). Singapore: Springer Singapore.
- [15] Aslam, R., Serdaroglu, G., Zehra, S., Verma, D. K., Aslam, J., Guo, L., ... & Quraishi, M. A. (2022). Corrosion inhibition of steel using different families of organic compounds: Past and present progress. *Journal of Molecular Liquids*, 348, 118373.
- [16] Li, W., Zhang, Z., Zhai, Y., Ruan, L., Zhang, W., & Wu, L. (2020). Electrochemical and computational studies of proline and captopril as corrosion inhibitors on carbon steel in a phase change material solution. *International Journal of Electrochemical Science*, 15(1), 722-739.
- [17] Chahmout, H., Ouakki, M., Sibous, S., Galai, M., Arrousse, N., Ech-Chihbi, E., ... & Cherkaoui, M. (2023). New pyrazole compounds as a corrosion inhibitor of stainless steel in 2.0 M H₂SO₄ medium: Electrochemical and theoretical insights. *Inorganic Chemistry Communications*, 147, 110150.
- [18] Guo, L., Tan, J., Kaya, S., Leng, S., Li, Q., & Zhang, F. (2020). Multidimensional insights into the corrosion inhibition of 3, 3-dithiodipropionic acid on Q235 steel in H₂SO₄ medium: a combined experimental and in silico investigation. *Journal of colloid and interface science*, 570, 116-124.
- [19] Parr, R. G., & Pearson, R. G. (1983). Absolute hardness: companion parameter to absolute electronegativity. *Journal of the American chemical society*, 105(26), 7512-7516.
- [20] Geerlings, P., De Proft, F., & Langenaeker, W. (2003). Conceptual density functional theory. *Chemical reviews*, 103(5), 1793-1874.
- [21] Foresman, J.B., Frisch, A. *Exploring Chemistry with Electronic Structure Methods*. Gaussian, Inc., Pittsburg, PA (USA) 1995.
- [22] Rajak, S. K., Islam, N., & Ghosh, D. C. (2011). Modeling of the chemico-physical process of protonation of molecules entailing some quantum chemical descriptors. *Journal of Quantum Information Science*, 1(02), 87.
- [23] Pauling, L. (1992). The nature of the chemical bond—1992. *Journal of Chemical Education*, 69(7), 519.
- [24] Abd El-Lateef, H. M., Abu-Dief, A. M., & Mohamed, M. A. (2017). Corrosion inhibition of carbon steel pipelines by some novel Schiff base compounds during acidizing treatment of oil wells studied by electrochemical and quantum chemical methods. *Journal of Molecular Structure*, 1130, 522-542.
- [25] Salman, T. A., Jawad, Q. A., Hussain, M. A. M., Al-Amiery, A. A., Mohamed, L., Kadhum, A. A. H., & Takriff, M. S. (2019). Novel ecofriendly corrosion inhibition of mild steel in strong acid environment: Adsorption studies and thermal effects. *International Journal of Corrosion and Scale Inhibition*, 8(4), 1123-1137.
- [26] Jamil, D. M., Al-Okbi, A. K., Al-Baghdadi, S. B., Al-Amiery, A. A., Kadhim, A., Gaaz, T. S., ... & Mohamad, A. B. (2018). Experimental and theoretical studies of Schiff bases as corrosion inhibitors. *Chemistry Central Journal*, 12, 1-9.
- [27] Ituen, E. B., James, A. O., & Akaranta, O. (2017). Fluvoxamine-based corrosion inhibitors for J55 steel in aggressive oil and gas well treatment fluids. *Egyptian journal of petroleum*, 26(3), 745-756.
- [28] Akpan, E. D., Singh, A. K., Lgaz, H., Quadri, T. W., Shukla, S. K., Mangla, B., ... & Ebenso, E. E. (2024). Coordination compounds as corrosion inhibitors of metals: A review. *Coordination Chemistry Reviews*, 499, 215503.
- [29] Mansour, A. A., Subbiah, K., Lgaz, H., Al-Hadeethi, M. R., Messali, M., Park, T., ... & Salghi, R. (2024). Investigating corrosion failure in N80 carbon Steel: Experimental and theoretical insights into isonicotinohydrazide derivatives as inhibitors in acidic conditions. *Inorganic Chemistry Communications*, 161, 112007.
- [30] Kavitha, V., Gunavathy, N., & Poovarasi, S. (2017). Efficacy of seed extracts of *Momordica charantia* on the corrosion inhibition of mild steel in 1n HCl medium using phytochemical screening, weight loss measurements and quantum chemical studies. *Ijariie*, 3, 1700-1712.
- [31] Pearson, R. G. (1969). Symmetry rule for predicting molecular structures. *Journal of the American Chemical Society*, 91(18), 4947-4955.

- [32] Hassouni, H. E., Elyousfi, A., Benhiba, F., Setti, N., Romane, A., Benhadda, T., ... & Dafali, A. (2022). Corrosion inhibition, surface adsorption and computational studies of new sustainable and green inhibitor for mild steel in acidic medium. *Inorganic Chemistry Communications*, 143, 109801.
- [33] Guo, L., Safi, Z. S., Kaya, S., Shi, W., Tüzün, B., Altunay, N., & Kaya, C. (2018). Anticorrosive effects of some thiophene derivatives against the corrosion of iron: a computational study. *Frontiers in chemistry*, 6, 155.
- [34] Ogede, R. O., Abdulrahman, N. A., & Apata, D. A. (2022). DFT computational study of pyridazine derivatives as corrosion inhibitors for mild steel in acidic media. *GSC Advanced Research and Reviews*, 11(3), 106-114.
- [35] Parr, R. G., Szentpály, L. V., & Liu, S. (1999). Electrophilicity index. *Journal of the American Chemical Society*, 121(9), 1922-1924.
- [36] Erazua, E. A., & Adeleke, B. B. (2019). A Computational Study of Quinoline Derivatives as Corrosion Inhibitors for Mild Steel in Acidic Medium. *Journal of Applied Sciences and Environmental Management*, 23(10), 1819-1824.
- [37] Eddy, N. O., Ameh, P. O., & Essien, N. B. (2018). Experimental and computational chemistry studies on the inhibition of aluminium and mild steel in 0.1 M HCl by 3-nitrobenzoic acid. *Journal of Taibah University for Science*, 12(5), 545-556.
- [38] Belghiti, M. E., Bouazama, S., Echihi, S., Mahsoune, A., Elmelouky, A., Dafali, A., ... & Tabyaoui, M. (2020). Understanding the adsorption of newly Benzylidene-aniline derivatives as a corrosion inhibitor for carbon steel in hydrochloric acid solution: Experimental, DFT and molecular dynamic simulation studies. *Arabian Journal of Chemistry*, 13(1), 1499-1519.
- [39] Li, X., He, J., Xie, B., He, Y., Lai, C., Wang, W., ... & Long, T. (2024). 1, 4-Phenylenediamine-based Schiff bases as eco-friendly and efficient corrosion inhibitors for mild steel in HCl medium: Experimental and theoretical approaches. *Journal of Electroanalytical Chemistry*, 955, 118052.
- [40] Chauhan, D. S., Srivastava, V., Joshi, P. G., & Quraishi, M. A. (2018). PEG cross-linked chitosan: a biomacromolecule as corrosion inhibitor for sugar industry. *International Journal of Industrial Chemistry*, 9, 363-377.